



Self-Calibrating Smart Mirror Design

Kaya MANOĞLU^{1*}, Barış TANER¹, Onursal ÖNEN¹, Serhan OZDEMİR¹

^{1*}Izmir Institute of Technology

IzTech Robotics Laboratory, Gülbahçe Mah., Urla, İzmir, Turkey

E-mail: kayamanoglu@iyte.edu.tr

Abstract

Self-Calibrating Smart Mirror is a source tracking mirror that is designed in Izmir Institute of Technology. This device uses ARM Cortex M4 chip to calibrate itself using the sound in environment and execute tracking operations to direct the mirror to the user. In this paper, mathematical model, calibration, experiments for sensor capabilities and tracking operations are presented and the prototype is expressed.

Keywords: Robotics, human-machine interface, sound tracking, source localization.

1. Introduction

Smart devices became common with the development of processors and sensors which are used in devices surrounding us and make them smarter every day with the need of easier interaction of human and machine. Smarter machines are designed to have the same communication methods of human that are visual, tactile, kinesthetic and auditory sensors [1] to be more sociable in the use of a human.

These communication methods can be used for increasing human perception in the slave environment that is interfaced by a haptic device [2] or to increase level of perception of the human commands by the machine [3]. As pointed in a research [4], some arcade games are using visual, infra-red, inertial measurement units and ultrasonic sensors to locate the users for shaping game inputs. Tactile and kinesthetic information in action and sports games as a reaction to the user by haptic devices are widely used application examples of communication between human and machine.

Other than sensing the motion of the human user by haptic devices, the motion inputs of the user can be detected by other means such as visual sensors using cameras [5], IR sensors [6] and auditory sensors [7]. Visual and IR sensors are commonly used sensor types for tracking environmental changes. These sensors are powerful considering the achievable resolution of the tracked workspace with respect to the auditory sensors; However, they are limited with the field of view and cannot locate outside of this region [1]. The field of view depends on parameters such as focal length of the lens, image sensor dimensions and distance to the measured plane [8]. In some vision applications, field of view can be enlarged using stereo vision techniques which include rectification of multiple images and matching them to create a larger field of view but this method requires

multiple cameras and greater computational costs [9].

One other way to locate user is using acoustic sensors. This method is used in real world by creatures to locate the sound source and give them a 360° field of view. It also allows them to locate sources that are obscured by any object that are not in the field of vision [1]. Researchers are using this method of localization in robots for tracking, socializing and navigating which has various application techniques.

In this paper, design of a smart mirror is described with its sensors, processor and mathematical model, which includes self-calibration, signal processing and source tracking in two-dimensional plane. The mirror is designed to be one Degree of Freedom (DoF) and uses an ARM Cortex M4 chip, which can locate the sound source using an array of microphones placed on the body.

2. Hardware used in Design

Device is composed of several electronics including processor, sensors and actuators. In this project an ARM based processor was selected and this chip was STM32F407VGT6. In the market, this chip is used by many third-party companies to build their own prototyping boards in which one of them is the STM32F4DISCOVERY Discovery board. This board allows users to easily develop applications with the STM32F407 high performance microcontrollers with ARM® Cortex®-M4 32-bit core. It includes an ST-LINK/V2 or ST-LINK/V2-A embedded debug tool, two ST MEM's digital accelerometers, a digital microphone, one audio DAC with integrated class D speaker driver, LEDs and push buttons and an USB OTG micro-AB connector [10].

A basic sound sensor card is used in this robotic application, which gives an analog output according to the sound level of the environment. The specifications of this sensor breakout are listed in Table 1.

Table 1. Sound sensor specifications

Frequency range	100 ~ 10,000 Hz
Sensitivity	- 46 ± 2.0, (0 dB = 1V/Pa) at 1K Hz
Power supply	5V maximum
Minimum Sensitivity to Noise Ratio	58dB for digital output

A light weight servo motor that can rotate approximately 180 degrees is placed beneath the mirror to rotate it around the azimuth axis. Body of the device is



made out of a foam-board for minimizing the reverberation problems.

2. Deciding the Geometry

Sensor placement plays an important role in product design and cabling since the way sensors are placed changes both signal transfer and acquisition problems with the sound tracking performance of the mirror. To declare it clearly, sound acquisition performance of microphones is affected by direction of the microphones. This fact about the sensors is an outcome of the experiment executed in this work. The experiment aims to measure sound level using four identical sound sensors in two different formations. One of the formations was placing them as a linear array and the other one was placing them radially as provided in Figure 1.

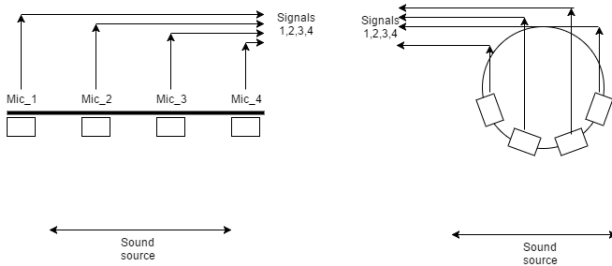


Fig.1. Test Formation for formation

The sensors in linear array set gives greater voltage values for the sounds sourced directly in front, however, other sensors in the same array set gives approximately close voltage levels that cannot be distinguished easily. The sensors in radial array set gives higher voltages once the sound sourced from the normal angle like the previous array set, however, it is easier to transfer signals from the sensors to the microchip due to the tight packing of the sensors.

In order to decide the geometry of the device, an experiment is designed and executed, especially for defining the microphone sensitivities at varying facing angles and distances. In this experiment, source is placed at different azimuth angles with varying distances from the sensor and sound level is measured. The azimuth angle and distances are given in Table 2.

Table 2 The Trial Table

Angle (degrees)	Distance (cm)
0	10, 20, 40, 60, 80
30	10, 20, 40, 60, 80
45	10, 20, 40, 60, 80
60	10, 20, 40, 60, 80
90	10, 20, 40, 60, 80

Sound source is measured for an average duration of 6-7 seconds for every combination of Table 2. Sine wave

of 500 Hz is used as a sound source. As additional information, it is known that the human sound is in a range of 85 to 1050 Hz, lowest frequency as a male bass sound and the highest as a female soprano. The results showed that the distance of the source has a significant effect in the sound level, as much as the microphone angle.

Measurements were mapped according to the distance and angle of the sound source with respect to the microphone. Five distinct measurements are executed for the angles of 0°, 30°, 45°, 60° and 90°, which include measurements of varying distances provided in Table 1. 0° is directly in front of the microphone and 90° is the perpendicular angle to the direct line of sight of the microphone. Tests are applied for every microphone and the measurements are illustrated only for one microphone.

Figures 2-6 provide the sound measurement of a microphone according to the different levels of distances for the same angle value, which are 0°, 30°, 45°, 60° and 90° respectively. Blue lines in these figures provide the information of the sound signal and the red lines give the measurement interval.

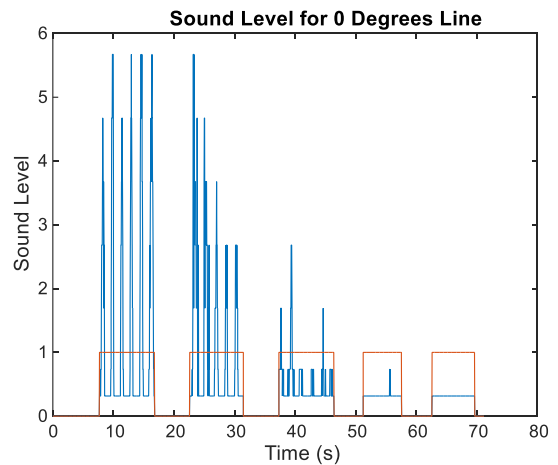


Fig.2. Sound level measurements for 0° azimuth angle

Fig. 2 illustrates the sound measurement of the microphone at 0° azimuth angle. At this angle, sound pressure is measured with the sensor and scaled to a 10-bit range. It is clear that sound level drops with increasing distance of the source, which is case for all other experiments executed for different azimuth angles, and maximum values are about 5.5 units.

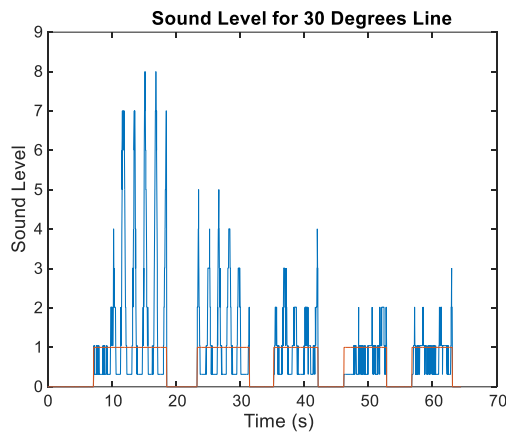


Fig.3. Sound level measurements for 30° azimuth angle

In Fig. 3, same sound measurement of the microphone at 30° azimuth angle is executed. In a 10-bit range, pressure levels are bounded between 0 and 9. It should be noted that, maximum sound level increases from 5.5 to 9 units for this angle compared to the one obtained in 0°.

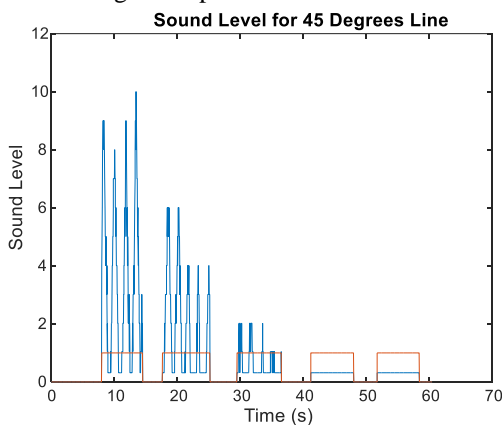


Fig.4. Sound level measurements for 45° azimuth angle

Fig. 4 provides the sound measurement of the microphone at 45° azimuth angle. In a 10-bit range, pressure values are bounded in a slightly greater region compared to the one acquired for 30°.

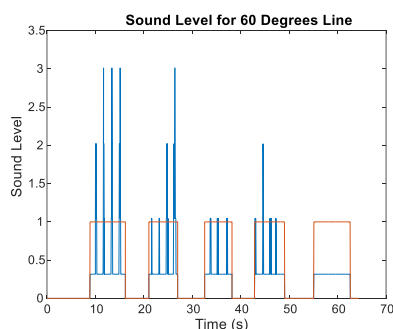


Fig.5. Sound level measurements for 60° azimuth angle

Fig. 5 designates the sound measurement of the microphone at 60° azimuth angle. In a 10-bit range, pressure values for different distances drop significantly to a range of 0.3 to 3 units.

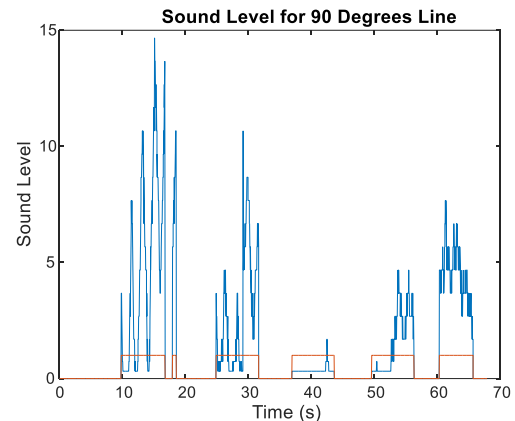


Fig.6. Sound level measurements for 90° azimuth angle

Fig. 6 marks the sound measurement of the microphone at 90° azimuth angle. It should be clarified that this is where the sound source is placed completely side of the microphone. At this angle device measures the source pressure level between the range of 0.3 and 15 units and measurements are not fitting in the expectations. To avoid any compromise due to the irregular behavior of the sensor at this azimuth angle, a foam body is designed to attenuate the signal coming from that angle.

Mapping of the Microphone in Polar Coordinates

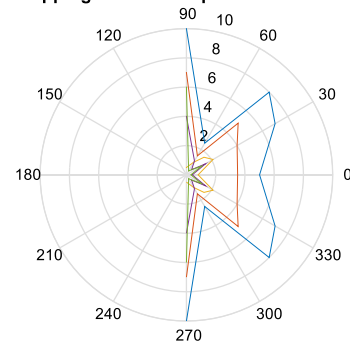


Fig.7. Sound level measurement in the sound sensor field of view

Fig. 7 connotes the overall ‘field of view’ of the sensor using polar coordinates. Blue, red, orange, green and purple lines show the sound pressure level of the source at 10, 20, 40, 60 and 80 cm distances respectively. As provided in this figure, microphone measures the sound pressure level of the source greater along 0° and smallest around 60°.

Using this knowledge, body is made of a foam material for minimizing the reverberation problem, which



is shaped as a half circle with openings in four different locations on the arc. These openings are specially designed for not allowing the microphones getting signals from the sides. Foam type materials are especially used for high frequency sound absorption above 2000 Hz, and it is possible to obtain better results by more proper material usage in the body. It is important to remark that this study is just a concept and in the process of development at the moment.

3. Localization Algorithm and Its Application

As expected, depending on the source location, different sound levels will be obtained by each microphone. Facing direction of each microphone is defined as a vector, which in the end will give the resultant vectors. It is said to be the logic of the system is based on the estimation of that resultant vector Fig. 8.

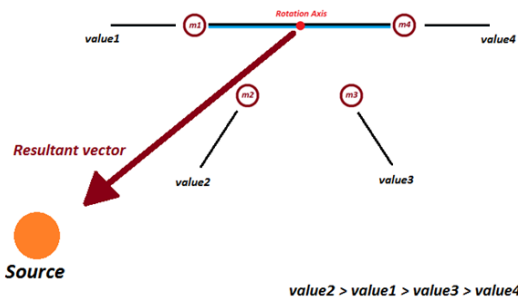


Fig.8. Sound levels from different source distances with varying microphone angles

A simple algorithm is developed for the system which is shown in Fig. 9.

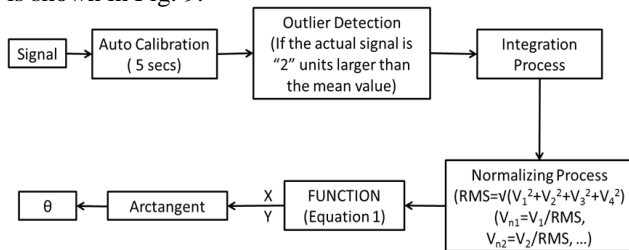


Fig.9. Diagram of the process

First step is the calibration process for the device. In order to do this, for 5 seconds, the device measures the average noise level of the room, which will be the mean value in the further calculations, to define the offset. This is illustrated in Fig. 10 with a block diagram.

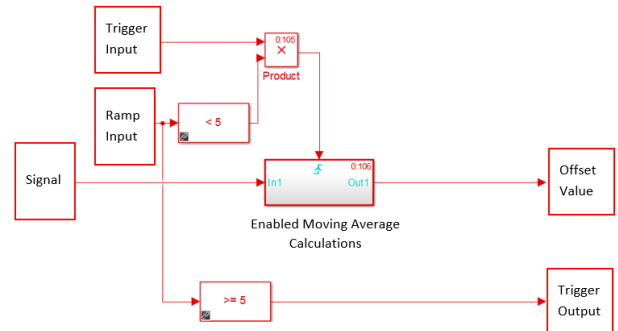


Fig.10. Block representation of auto-calibration function

Trigger and ramp input work together to enable the moving average calculations, which works for 5 seconds in this case, and at the end of this 5 second time interval, block releases the value as offset value. Trigger output in this sub-system is used as a switch to allow calibrated signal to be used in further calculations. After 5 seconds, when the calibration is completed, the incoming signals are being started to be analyzed. Firstly, threshold value is used to allow calibrated signals that are powerful enough to be analyzed. This data is taken into the integration process in a specified time range which is between the rising and the dropping edges of the curve. This process is connoted in Figure 11.

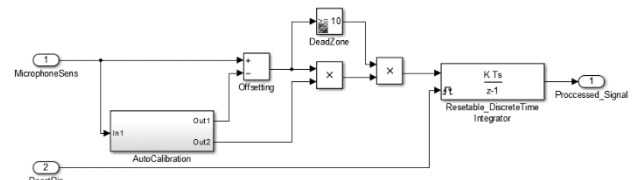


Fig.11. Block representation of signal processing phase

The normalizing step follows the integration procedure, which allows us to assign the value of “1” to the microphone signal that is the greatest and the other microphone values take values according to their value. This is provided in Fig. 12. To normalize signals their root mean square is calculated and every signal is then divided to this value. This is explained in Eq. 1.

$$N_j = \frac{S_j}{\sqrt{\sum_{i=1}^4 S_i^2}}, \quad j = 1,2,3,4 \quad (1)$$

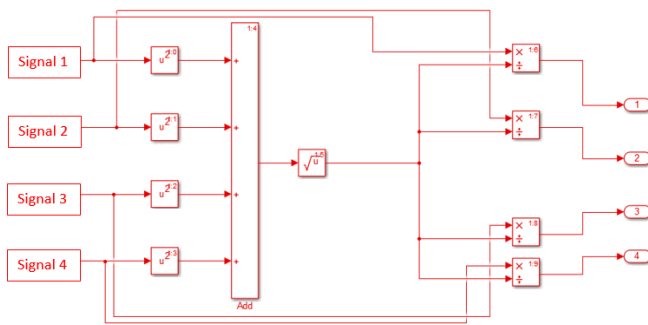


Fig.12. Block representation of normalization process

After this step, we are applying a function to the obtained microphone values to determine the direction of the sound source by distinguishing the x and y components of the required resultant normal vector using Eq 2. When x and y components are obtained, it becomes very simple to convert this to an angle of θ , by using the arctangent function.

$$\begin{bmatrix} X_{SS} \\ Y_{SS} \end{bmatrix} = \begin{bmatrix} \sum_{i=1}^4 (\text{Microphone Value})_i * \cos\theta_i \\ \sum_{i=1}^4 (\text{Microphone Value})_i * \sin\theta_i \end{bmatrix} \quad (2)$$

The code generation is executed using the Waijung module in Matlab Simulink. This module is third-party software that includes blocks for different operations such as mathematical operations, logic operations and etc. Using this software created model is downloaded in discovery board.

Microphones are placed on top of the mirror in a radial array and body of the mirror assembly is made out of foam due to previously designated experimental results. Servo motor is placed in the bottom part of the mirror assembly and the mirror is attached to the servo motor. The prototype is illustrated in Fig. 13.

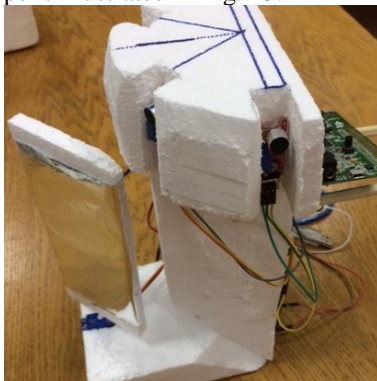


Fig.13. Experimental prototype of sound tracking mirror

4. Results

After manufacturing the smart mirror, simple tests are conducted to see if the algorithm is works as expected on the STM32F4 chip and prototype follows the sound source on 2-D plane. This is executed by clapping hand

close to the smart mirror at angles ranges from 0° to 180° . To visualize the working principle sound level measurements of the 3rd microphone is acquired from the raw signal stage to the processed signal stage. Fig. 14 gives the raw data that is acquired by the 3rd microphone. Before 5th second microphone receives only the surrounding sources that creates the noise. After 8th second microphone receives the clapping sound.

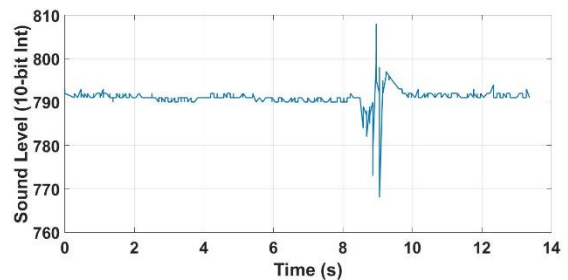


Fig. 14. Raw sound signal graph

This signal is then calibrated so that surrounding sound is eliminated. After calibration, the output signal of the calibration stage is integrated to store the value that will be used in calculation of angular position. Result of the integration of 3rd microphone signal is given in Fig.15.

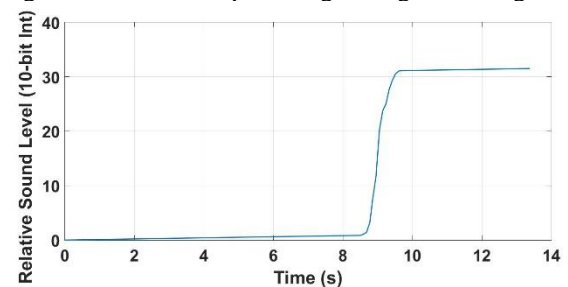


Fig. 15. Calibrated and processed signal

All four signals are run into the same algorithm, and the resultant signals of every one of them is sent to normalization stage but in results section and result of the normalization is given in Fig. 16. As given in Fig. 16 with the increasing value of the integration coming from the 3rd microphone, normalized signal of line of the 3rd microphone goes to one, while the others reduces in value. The yellow line in Fig 16. shows the value of the line of 3rd microphone.

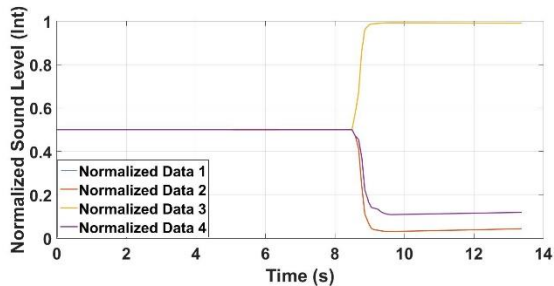


Fig. 16. Signals after normalization

After the normalization process, x and y components of the sound source vector is used to calculate the angular position of the sound source with respect to the mirror origin in 2-D plane. This is provided is Fig. 17.

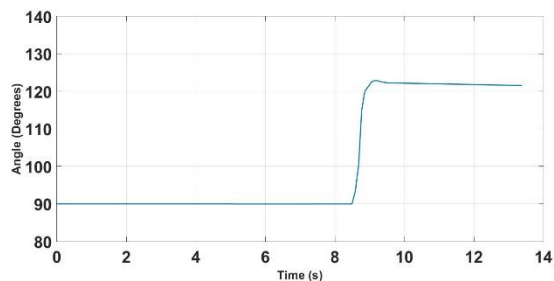


Fig. 17. Angle calculation graph

As given in Fig. 17 a series of clap that is close to the 3rd microphone, which is placed at 120°, results in a calculated angle of 124°, with an error of 4°.

5. Comments and Conclusion

In this paper, a 1 DoF smart mirror is designed using 4 radially placed sound sensors. The purpose of this mirror is to construct a system, which can be used in robotic systems that interacts with humans. The controller of the system is designed over the STM32F4 Discovery board and the system is deployed on the chip using Matlab.

In preliminary design, microphone field of view is revealed to be used in design of the mirror and sensors are placed using this information. Field of view experiments show that there is an unexpected rise in the sound level at 90° angle, where sound level is measured to be the largest. To eliminate this problem sensors are placed in a foam head that reduces the sound level coming from this angle. After this stage, control algorithm is deployed in the discovery board.

In this prototype, an integration is executed for every signal and the resultant signals are normalized. This is used to store the positional data, however, after several repetitions of localization, integrated values that are feed in the normalization get high values. This creates a problem of latency once another sound source transmits

sound. In this particular case, device turns to the new source slowly, since integration of the acquired sound signal takes time to reach the previously integrated value. To overcome that problem, smart mirror has to be reset, which is done by a digital input given by the user.

Even though this system is designed as a smart mirror to interact with humans, it may very well be equipped with other device or objects along with a different line of sensors, oriented towards commercial or industrial purposes.

It should be mentioned that the curvilinear deployment of sound sensors may also be regarded as a distributed sensor network, whose detailed analysis is left for a later research. But it is seen that as the number of sensors is increased, localization resolution is also on the rise.

References

- [1]. Murray, John C., Harry Erwin, and Stefan Wermter. "Robotics sound-source localization and tracking using interaural time difference and cross-correlation." *AI Workshop on NeuroBotics*. 2004.
- [2]. Taner, B., and M. İ. C. Dede. "Image Processing Based Stiffness Mapping of a Haptic Device." *New Advances in Mechanisms, Mechanical Transmissions and Robotics*. Springer International Publishing, pages 447-454, 2017.
- [3]. Web, <http://web.media.mit.edu/~cynthiab/Papers/Breazeal-TICS02.pdf>
- [4]. Breazeal, Cynthia, et al. "Learning from and about others: Towards using imitation to bootstrap the social understanding of others by robots." *Artificial life* 11.1-2, pages 31-62, 2005.
- [5]. Wermter, Stefan, et al. "Towards multimodal neural robot learning." *Robotics and Autonomous Systems* 47.2, pages 171-175 2004.
- [6]. Zhang, Zhengyou. "Microsoft kinect sensor and its effect." *IEEE multimedia* 19.2 (2012): 4-10.
- [7]. Nakadaij, Kazuhiro, et al. "Real-time tracking of multiple sound sources by integration of in-room and robot-embedded microphone arrays." *Intelligent Robots and Systems, 2006 IEEE/RSJ International Conference on*. IEEE, 2006.
- [8]. Web, <http://www.inf.u-szeged.hu/~kato/teaching/computervision/02-CameraGeometry.pdf>
- [9]. Web, <http://vision.deis.unibo.it/~smatt/Seminars/StereoVision.pdf>
- [10]. Web, http://www.st.com/content/ccc/resource/technical/document/data_brief/09/71/8c/4e/e4/da/4b/fa/DM00037955.pdf/files/DM00037955.pdf/jcr:content/translations/en.DM00037955.pdf.